Excitons in resonant coupling of quantum wells

A. M. Fox, D. A. B. Miller, G. Livescu,* J. E. Cunningham, J. E. Henry, and W. Y. Jan
AT&T Bell Laboratories, Crawfords Corner Road, Holmdel, New Jersey 07733
(Received 30 October 1989)

We examine, experimentally and theoretically, the effects of excitons in optical measurements of resonant coupling of quantum wells. We find that the exciton line splittings do not correspond directly to the underlying electron levels, which leads to differences in the bias fields for resonance of, e.g., ~10%. We construct a variational model of excitons in coupled wells and successfully compare this model with measured splittings near the resonance between the first and second electron levels of adjacent wells, deducing the actual conditions for coupling of the "bare" electron levels.

Resonant coupling of levels in adjacent quantum wells is a subject of considerable recent interest.[1–12] This phenomenon is a useful tool for understanding the physics of tunneling in layered semiconductors, and both this physics and the resonantly coupled structures themselves are important for many optical and electronic devices. One consequence of such resonant level coupling is splitting of the levels. To date, these splittings have only been observed in optical spectra, in which excitonic peaks split into doublets as a bias electric field perpendicular to the layers adjusts the relative positions of the levels in adjacent wells.[3–7] The purpose of this paper is to explain the effects of excitons in such resonant coupling. In particular, we show that the exciton splittings do not occur at the same field as the "bare" electron (or hole) level resonances, nor is the splitting the same size in principle. The reason is that the Coulomb interaction between the electron and the hole in the exciton can be strong enough to mix the coupled single-particle states. We measure this effect by comparing two different exciton splittings corresponding to the same coupled electron levels, and by constructing a variational model for excitons in coupled wells, we compare experiment and theory. Hence we can deduce the true electron level coupling.

In Fig. 1(a) we sketch the conduction and valence bands of a multiple-quantum-well structure when an electric field F has been applied to align the $n=1$ and electron states ($e1$ and $e2$) of adjacent wells. For clarity only three wells are shown, and we consider only the $n=1$ heavy-hole state (hh1) in the valence band. Throughout this paper we concentrate on two optical transitions: $H11$ from hh1 to $e1$, and $H12$ from hh1 to $e2$. The latter transition is symmetry forbidden at zero field, but not at the fields of interest here. The effects we will discuss are general to any transition involving either the first or second electron sublevels.

In Fig. 1(b) we sketch the field-dependent energies of the $H11$ and $H12$ transitions. Because the barriers separating the wells are thin, the electron wave functions are not totally localized in any particular well, but leak weakly through the barrier into nearest-neighbor wells. This means that there is a small but finite overlap between hole states localized in one well and the electron states in adjacent wells. We must therefore consider both spatially direct (intrawell) and spatially indirect (interwell) transitions.[13,6,7] At moderate applied fields there are thus three transitions to be considered for each of $H11$ and $H12$ in the three-well structure of Fig. 1(a): the strong intrawell transition indicated by the solid lines in

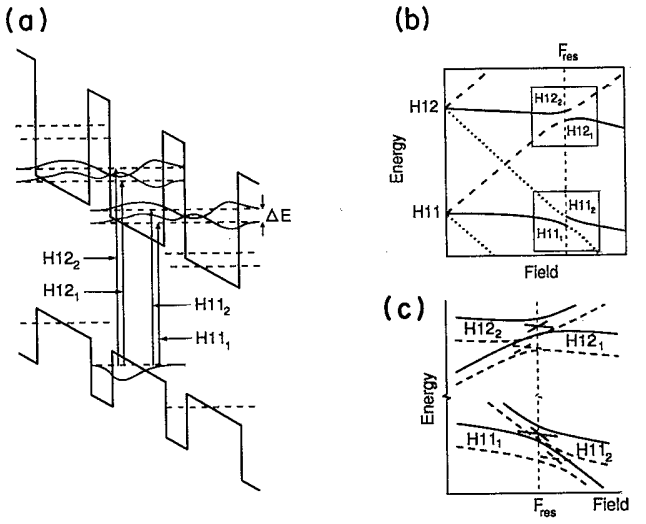

FIG. 1. (a) Schematic band diagram of three wells from within a resonantly coupled multiple-quantum-well structure. The $H11$ and $H12$ intrawell doublet transitions are indicated, together with the hh1 and mixed $e1$-$e2$ wave functions. The el-$e2$ splitting ΔE is exaggerated for clarity. (b) Field dependence of the $H11$ and $H12$ optical transition energies. Intrawell transitions are indicated by the solid lines, while interwell transitions are shown by broken and dotted lines. (c) Expanded version of (b) showing the detailed field-dependent optical transition energies close to resonance with (dashed lines) and without (solid lines) the electron-hole Coulomb interaction.

Fig. 1(b), and the two weak interwell transitions indicated by the dotted and dashed lines.

The situation changes drastically when the resonant field F_{res} is reached. The unperturbed $e1$ and $e2$ levels of adjacent levels are now degenerate, and the coupling through the barrier leads to the formation of two delocalized states split in energy by ΔE with the wave functions as sketched in Fig. 1(a). These two states have approximately equal overlap with the hh1 hole wave function, so there are now two strong intrawell transitions for each of $H11$ and $H12$, as indicated by the vertical arrows in Fig. 1(a). We label these intrawell doublets as follows: $\{H11_1, H11_2\}$ and $\{H12_1, H12_2\}$. The subscript refers to the number of nodes in the electron wave function. Note that at resonance the $H11$ and $H12$ transitions involve the same electron wave functions, except that $H11$ is sensitive to the $n=1$-like part of the mixed wave functions, while $H12$ is sensitive to the $n=2$-like part. When the applied field is increased beyond F_{res}, the $e1$ and $e2$ states again become localized predominantly in just one well, and so we return to the usual situation where there is only one intrawell transition for $H11$ and $H12$.

We now turn to reconsider the behavior close to F_{res} in more detail. Both transitions exhibit anticrossing at F_{res}. The field-dependent splitting of the coupled $e1$-$e2$ states is minimum at F_{res}, and its magnitude depends critically on the coupling strength through the barrier. In Fig. 1(c) we sketch the field-dependent transition energies close to F_{res}. In an optical experiment holes are generated simultaneously with electrons, and we have to consider the effects of the electron-hole Coulomb attraction. On a microscopic scale, the presence of the holes can lead to the formation of excitons,[6,7,13–16] while on a macroscopic scale, the holes can cause space charge effects.[17] The solid lines in Fig. 1(c) show the transition energies when the electron-hole interaction is neglected. The splitting of the $H11$ and $H12$ doublets depends entirely on the electron states and has a minimum at F_{res}, which is the same for both transitions in this approximation. The dashed lines show what happens when the Coulomb interaction is included. The transition energies are now shifted down by the exciton binding energies. Above or below F_{res}, the intrawell excitons have a larger binding energy than the interwell excitons because of the indirect spatial nature of the latter. Since the intrawell and interwell character of the components of the doublets changes on sweeping the field through F_{res} [see Fig. 1(b)], so too must the exciton binding energy associated with each transition. Figure 1(c) shows that this *increases* the field for minimum level separation for the $H11$ transition, and *reduces* it for the $H12$ transition. *Neither* transition follows the true splitting of the electron levels, which can only be deduced from modeling the excitonic effects (see below).

We grew a sample consisting of 80 periods of nominally undoped $GaAs/Al_{0.33}Ga_{0.67}As$ by molecular-beam epitaxy. The quantum wells were grown as the intrinsic region of a *p-i-n* diode on an N^+-doped GaAs substrate, *with* doping densities in the *p* and *n* regions of 5×10^{17} cm^{-3}. The nominal GaAs quantum-well width L_w and $Al_{1-x}Ga_xAs$ barrier width L_b were 95 and 35 Å, respectively. X-ray diffraction measurements gave $L_w=84$ Å and $L_b=31$ Å. The same x-ray data gave the Al concentration of the barrier material to be 33%, which checked well against the optical-absorption edge of the barriers.

Figure 2 shows representative photocurrent spectra measured at 30 K using a tungsten-lamp light source. We consider first the optical transitions close to the fundamental absorption edge shown in Fig. 2(a). At 5.8 V the $n=1$ heavy- and light-hole exciton transitions are well resolved. Between 6.2 and 7.5 V the heavy-hole absorption line breaks into a doublet with field-dependent splitting and relative amplitude ratio. Arrows indicate the deconvolved energies of the two components of the doublet. The lower-energy component is the $H11_1$ transition, while the higher energy component is $H11_2$. Below 7.0 V the $H11_1$ transition dominates the spectrum, but above 7.0 V it is the $H11_2$ transition which now dominates. At 7.0 V the two transitions have approximately equal amplitude and a minimum energy separation of ~4.5 meV. The light-hole line is also noticeably broadened at this voltage. The resonant anticrossing is clearer when we plot the deconvolved transition energies against voltage in Fig. 3(a).

In Fig. 2(b) we show photocurrent spectra of the $H12$ transition. Below resonance the lower-energy $H12_2$ transition is the stronger component of the resonant doublet, and the oscillator strength switches over on scanning through the resonance [see Fig. 2(b)]. Figure 3(b) shows the energies of the two transitions for applied bias between 5 and 8 V. The anticrossing is evident, with a minimum splitting of 5.8 meV at 6.4 V.

On comparing the two anticrossings, we immediately notice that the field dependence of the splittings is different. If we were to ignore the Coulomb interaction we might expect that the splittings would be identical, since both originate from the same electron resonance. This is not true, however, if we include the Coulomb interaction, as explained above and in Fig. 1(c). The experimental results clearly show that the field for minimum

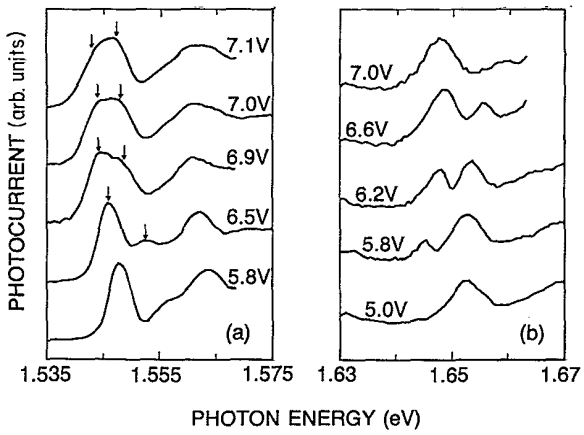

FIG. 2. Voltage-dependent photocurrent spectra of the $GaAs/Al_{0.33}Ga_{0.67}As$ multiple-quantum-well structure at 30 K: (a) close to the fundamental absorption edge, and (b) near the $H12$ transition.

splitting is greater in the $H11$ transition than for $H12$.

To test our model quantitatively, we calculated the field dependence of the exciton energies variationally. We use the following Hamiltonian:

$$H=-\frac{\hbar^2}{2\mu_{xy}}\nabla_{xy}^2-\frac{\hbar^2}{2m_e}\frac{\partial^2}{\partial z_e^2}-\frac{\hbar^2}{2m_h}\frac{\partial^2}{\partial z_h^2}-\frac{e^2}{4\pi\varepsilon_0\varepsilon_r r}$$
$$\pm eFz_{e,h}+V_{e,h}(z_{e,h})\,. \tag{1}$$

The subscripts e and h and the signs $-$ and $+$ refer to electrons and holes, respectively, for the field direction as in Fig. 1(a), z is the direction perpendicular to the layers, $r=[x^2+y^2+(z_e-z_h)^2]^{1/2}$, μ_{xy} is the x-y plane reduced effective mass, $m_{e,h}$ is the particle effective mass, and $V_{e,h}$ is the quantum-well potential. We first solve for the quasi-bound states without the Coulomb interaction and the x-y plane kinetic energy.[18] We use the tunneling resonance technique to find the energies and normalized wave functions of the two split electron states near the resonance: $\Psi_{e_1}(z_e)$ and $\Psi_{e_2}(z_e)$. The subscripts 1 and 2 refer to the number of wave-function nodes. The energy and wave function $\Psi_h(z_h)$ of the hh1 sublevel are found similarly.

The Coulomb interaction and x-y kinetic energy are included variationally. We allow for possible Coulomb mixing of the nearly degenerate electron wave functions by using the following (orthogonal) trial wave functions:

$$\Psi_+=[\alpha\Psi_{e_1}+(1-\alpha^2)^{1/2}\Psi_{e_2}]\Psi_h\Phi_{1s}(\lambda)\,,$$
$$\Psi_-=[-(1-\alpha^2)^{1/2}\Psi_{e_1}+\alpha\Psi_{e_2}]\Psi_h\Phi_{1s}(\lambda)\,, \tag{2}$$
$$\Phi_{1s}(\lambda)=\left[\frac{2}{\pi}\right]^{1/2}\frac{1}{\lambda}\exp\left[\frac{-(x^2+y^2)^{1/2}}{\lambda}\right],$$

where $(1-|\alpha|)$ is the mixing amplitude and λ is the x-y plane $1s$ exciton diameter. α and λ are varied to minimize the energy of the lower level, and then λ is reminimized to find the energy of the other level. With real Ψ_+ and Ψ_-, α must be real with modulus ≤ 1. The mixing is caused by the tendency of the localized holes to attract the electrons to their own well. Intuitively, we expect $|\alpha|$ to be close to unity except near $F_{\rm res}$.

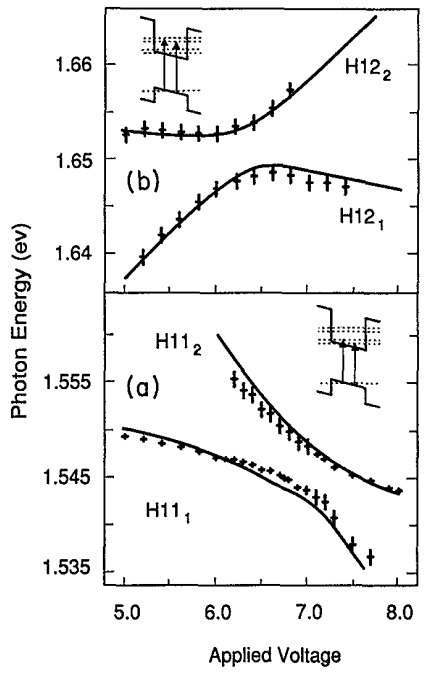

FIG. 3. Measured exciton energies at 30 K for (a) the $H11$ and (b) the $H12$ optical transitions. The solid lines show the results of a variational calculation of the exciton transition energies.

The curves plotted over the data in Figs. 3(a) and 3(b) show the results of the calculation. The same set of parameters was used for both sets of curves. The best fit material parameters used were $L_w=89$ Å, $L_b=35$ Å, Al concentration $=0.33$, $\Delta E_c:\Delta E_v=67:33$. The effective masses used were $m_e=0.0665$, $m_h=0.34$, $\mu_{x,y}=0.0415$ for GaAs, and $m_e=0.16$, $m_h=0.76$ for the $Al_{1-x}Ga_xAs$. We use an averaged material-independent dielectric constant of 12.15. The band gaps used were 1.522 eV for GaAs and 1.934 eV for $Al_{0.33}Ga_{0.67}As$. GaAs conduction-band nonparabolicity was included according to Eq. (64) of Ref. 19. The value used for the built-in voltage of the diode was -1.65 V. With these parameters we were able to obtain a reasonable fit to the transition energies of all the resolved heavy-hole transitions at 0 and 5 V, and also to the Stark shift of the heavy-hole exciton at room temperature for voltages up to 15 V. Away from resonance the $H11$ intrawell exciton binding energy is calculated to be 8.0 meV at 5.8 V, which compares to 3.7 meV for the interwell excitons. The results accurately reproduce the shift in field for minimum splitting for the two transitions, and also give fairly close agreement with the absolute magnitude of the splitting over the entire voltage range studied. The calculated minimum splittings are similar for the two transitions, although experimentally they differ by 25%. The mixing amplitude $(1-|\alpha|)$ is small except near resonance, with a maximum value of 15% for the $H11$ transition, but only 2% for $H12$. We calculate that the actual value of ΔE for the bare electron levels is 5.5 meV at 6.7 V. Thus the excitonic corrections shift the resonant fields by $\pm 5\%$.

We conclude that great care needs to be taken when interpreting optical resonant tunneling measurements: the field dependence of the exciton line splitting corresponds neither conceptually nor quantitatively with the underlying single-particle-state splitting. From Fig. 1(c) one can estimate that the fractional field shifts will be over 20% for some samples. We have quantified these effects for an electron resonance in two specific optical transitions, but our conclusions have general applicability to all interband optical resonant tunneling experiments that measure exciton peaks. This applies equally well to both elec-

tron and hole resonances in superlattices or symmetric double-well structures, and it also applies to ground-to-ground resonant coupling in asymmetric quantum wells. The effects will be most pronounced in samples where the difference in the binding energy of interwell and intrawell excitons is comparable to ΔE. We believe that our conclusions will be important for an improved understanding of optical resonant tunneling experiments, as well as in the design of coupled quantum-well electroabsorptive devices.

We would like to acknowledge helpful discussions with S. L. Chuang.

*Present address: AT&T Bell Laboratories, Murray Hill, NJ 07974.

[1]R. F. Kazarinov and R. A. Suris, Sov. Phys. Semicond. **5**, 707 (1971) [Fiz. Tekh. Poluprovodn. **5**, 797 (1971)].

[2]F. Capasso, K. Mohammed, and A. Y. Cho, Appl. Phys. Lett. **48**, 478 (1986); IEEE J. Quantum Electron. **QE-22**, 1853 (1986).

[3]T. Furuta, K. Hirakawa, J. Yoshino, and H. Sakaki, Jpn. J. Appl. Phys. **25**, L151 (1986).

[4]H. Q. Le, J. J. Zayhowski, and W. D. Goodhue, Appl. Phys. Lett. **50**, 1518 (1987).

[5]M.-H. Meynadier, R. E. Nahory, J. M. Worlock, M. C. Tamargo, J. L. de Miguel, and M. D. Sturge, Phys. Rev. Lett. **60**, 1338 (1988).

[6]J. E. Golub, P. F. Liao, D. J. Eilenberger, J. P. Harbison, L. T. Florez, and Y. Prior, Appl. Phys. Lett. **53**, 2584 (1988).

[7]Y. Tokuda, K. Kanamoto, N. Tsukada, and T. Nakayama, J. Appl. Phys. **65**, 2168 (1989); Appl. Phys. Lett. **54**, 1232 (1989).

[8]K. K. Choi, B. F. Levine, C. G. Bethea, J. Walker, and R. J. Malik, Phys. Rev. Lett. **59**, 2459 (1987).

[9]S. Tarucha and K. Ploog, Phys. Rev. B **39**, 5353 (1989).

[10]H. Schneider, K. von Klitzing, and K. Ploog, Superlatt. Microstruct. **5**, 383 (1989); H. Schneider, W. W. Ruhle, K. von Klitzing, and K. Ploog, Appl. Phys. Lett. **54**, 2656 (1989).

[11]G. Livescu, A. M. Fox, D. A. B. Miller, T. Sizer, W. H. Knox, A. C. Gossard, and J. H. English, Phys. Rev. Lett. **63**, 438 (1989).

[12]D. Y. Oberli, J. Shah, T. C. Damen, C. W. Tu, T. Y. Chang, D. A. B. Miller, J. E. Henry, R. F. Kopf, N. Sauer, and A. E. DiGiovanni, Phys. Rev. B **40**, 3028 (1989).

[13]Y. J. Chen, E. S. Koteles, B. S. Elman, and C. A. Armiento, Phys. Rev. B **36**, 4562 (1987).

[14]S. R. Andrews, C. M. Murray, R. A. Davies, and T. M. Kerr, Phys. Rev. B **37**, 8198 (1988).

[15]J. Lee, M. O. Vassel, E. S. Koteles, and B. Elman, Phys. Rev. B **39**, 10 133 (1989).

[16]I. Galbraith and G. Duggan, *Topical Meeting on Quantum Wells for Optics and Optoelectronics, 1989 Technical Digest Series* (Optical Society of America, Washington, D. C., 1989), Vol. 10, Paper TuE2-1, p. 158.

[17]R. Sauer, K. Thonke, and W. T. Tsang, Phys. Rev. Lett. **61**, 609 (1988).

[18]D. A. B. Miller, D. S. Chemla, T. C. Damen, A. C. Gossard, W. Wiegmann, T. H. Wood, and C. A. Burrus, Phys. Rev. B **32**, 1043 (1985).

[19]J. S. Blakemore, J. Appl. Phys. **53**, R123 (1982).